Egypt. J. Chem. **Vol. 62**, No.1 pp. 97 - 108 (2019)

Molecular Engineering of D-π-A Based on 1,3-Dimethoxybenzene π Spacer for Dye-Sensitized Solar Cells

Walid Sharmoukh[1]*, Zeinab M. Hassan[2], Basant A. Ali[3], Mohamed M. Elnagar[1], Hanan A. Mousa[1], Ammar A. Labib[1]

[1]National Reseach Centre, Inorganic Chemistry Department, Tahrir St, Dokki, 12622 Giza, Egypt.

[2]Fayoum University, Faculty of Sciences, Chemistry Department, Egypt.

[3]Energy Materials Laboratory (EML), School of Sciences and Engineering, The American University in Cairo, New Cairo 11835, Egypt.

A NEW organic sensitizer incorporating D35 as a donor unit, 1,3-dimethoxybenzene as a new π- linker that can be anchored to the TiO_2 surface, was synthesized and characterized by UV–Vis, NMR and Mass spectroscopy. The photophysical and electrochemical properties as well as photovoltaic performance of this dye have been studied to evaluate the impact of new π- linker on the power conversion efficiency (PCE) based device. The geometrical configuration of the sensitizer was optimized by density functional theory (DFT) calculations to gain a deep insight into the molecular structure and the electronic properties. Photovoltaic measurements of the present sensitizer in a DSSC configuration was found to show JSC = 4.0 mA cm^{-2}, VOC = 610 mV, FF = 0.53 and η = 1.3% under standard AM 1.5 G illumination.

Keywords: Photosensitizers, Cobalt electrolyte, TD-DFT; DSSC, π- linker

Introduction

The progress of solar energy technologies offers a hopeful solution to address the global energy crisis. In this respect, dye-sensitized solar cells (DSSCs) are one of the most effective alternate solar cell technologies owing to their cost effective and eco-friendly features [1-5]. Typical DSSC devices comprise a semiconductor photoanode (typically TiO_2), a dye sensitizer, an electrolyte and a counter electrode [6]. The dye sensitizer is a crucial component for harvesting sun light and power conversion efficiency (PCE) [7]. In the past decade, researchers have focused on developing new and highly efficient sensitizers. Among them metal-free organic sensitizers have a great deal of interest because of the structural diversity, understandable design, facile molecular tuning, high molar extinction coefficients and tunable photophysical properties [8, 9]. High- efficient organic sensitizers frequently feature a donor--bridge-acceptor (D–π–A) motif. The electronic interaction between donor (D) and acceptor (A) promotes efficient intramolecular charge transfer (ICT) that harvest sunlight for photon-to-electron conversion [10-12].

The studies on D–π–A organic dyes reveal that π-spacer has a significant role in facilitating the electron transfer, regulating the HOMO-LUMO energy gap, extending the absorption range of the sensitizers. Common π-spacers such as phenyl, thiophene, and furan ring have been investigated to increase dyes' light harvesting capacity and hinder the back electron transfer causing higher performance of their DSSC devices [11, 13, 14].

Regards to donors, several electron rich units such as indoline[15], coumarins [16], phenothiazine [17], Dithienylpyrrole [18], triphenylamines [19-21] have been successfully utilized. Among them, triphenylamine (TPA) moiety can suppress the dye aggregation due to its non-planar structure. Therefore, TPA-based organic sensitizers have revealed great potential in the manufacturing of highly efficient DSSCs devices [22, 23]. The cyanoacrylic acid, as the acceptor group, mainly achieves the prerequisite of an electron acceptor as well as providing the carboxylic acid group for binding the dye to the semiconductor surface [24, 25].

The optimization of the sensitizers is generally based on *"guess-and-check"* method. In this

*Corresponding author e-mail: walidm@kth.se

DOI: 10.21608/EJCHEM.2018.4249.1376

respect, density functional theory (DFT) and time-dependent density functional theory (TD-DFT) calculations can afford an excellent expectation of the sensitization properties of the sensitizers upon the variation of their structure [26].

In the meanwhile, much effort is still needed for the design and synthesis of novel organic sensitizers with broad and efficient optical absorption as well as narrow band-gaps for DSSCs fabrication. Herein, the influence of introducing 1,3-dimethoxybenzene as a new π- linker on the optical and electrochemical properties as well as PCE of D–π–A organic sensitizer incorporating D35 as an electron donor unit is systematically investigated. Furthermore, DFT and TD-DFT calculations were elaborated in order to understand the major properties related to the geometry of the dye. The molecular structure of the new synthesized dye is shown in Fig. 1.

Experimental

DFT Calculations

The studied dye was optimized to its lowest energy using DFT [27] as implemented in Gaussian 09 software package [28]. The level of the performed calculation was the hydride three-parameter density functional method (B3LYP) [29] which contains the gradient exchange correction function (B3) along with the correlation functional [30, 31] this level of calculations was proved to provide energetic and geometrical parameters better than other methods [29, 32]. cc-pVDZ [33] was used as the bases set for the calculation of the optimization due to the large steric of the molecule [34, 35].

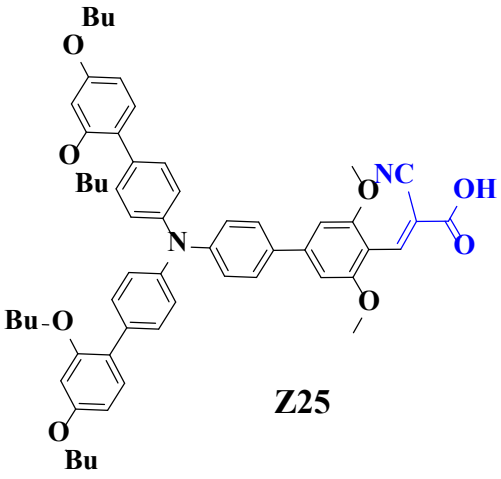

Fig. 1. Molecular structure of the synthesized dye

Furthermore, the basis set 6-31+G was employed for TD-DFT calculation in order to generate the first 10 excited states and the total energy of the molecules. 6-31+G is suitable for molecules that include large number of atoms (more than 130 atoms) [36]. Visualization of the data was performed using Chem Craft 1.6 [37] and GaussView 5.0 [38] software. The total energy of the optimized dye, the monovalent cation and monovalent anion were calculated using the single point calculation on the same optimized geometry. Electron affinity (EA) was calculated as the difference between the total energy of the neutral dye and that of the monovalent anion (by removing the hydrogen atom in the carboxylic group). The ionization potential 18 was calculated as the difference between the total energy of the neutral dye and that of the monovalent cation. Excitation binding energy ($E_{excitation}$) was calculated as the difference between the LUMO and HOMO in both DFT and TD-DFT calculations [39]. Normalized excitation binding energy (N_{Ex}) was calculated as the excitation binding energy divided by the energy of band gap, to be able to get the effect on excitation binding energy independent to the value of the bandgap [40]. Light harvesting efficiency (LHE) of the studied dyes was calculated as [41]:

$$LHE = 1\text{-}10^{-f} \quad (1)$$

(Gaussian 09, #28)

Experimental Materials and Synthesis

Chemicals and Solvents

All solvents were of HPLC grade quality and used without further purification. Reactions were carried out under a dry nitrogen atmosphere. All chemicals including 4-bromo-2,6-dimethoxybenzaldehyde, palladium(II) acetate, 2-cyanoacetic acid, tri-o-tolylphosphine, phosphoursoxychloride, 2,2′-bipyridine, cobalt chloride hexahydrate ($CoCl_2.6H_2O$), nitrosyl tetrafluoroborate ($NOBF_4$), ammonium hexafluorophosphate (NH_4PF_6) and tetrabutylammonium hexafluorophosphate ($TBAPF_6$) were purchased from Sigma-Aldrich, Acros or Alfa-Aesar. Electrolyte components–$Co(bpy)_3$ $(PF6)_2$ and $Co(bpy)_3$ $(PF6)_3$ were synthesized according to the literature [42].

Structural, optical and electrochemical characterization

^1H and ^{13}C NMR spectroscopy study was conducted on Bruker 500 MHz instruments by using the residual signals for $CDCl_3$ at δ = 7.26 ppm and 77.0 ppm as internal references for

^{1}H and ^{13}C, respectively. PerkinElmer Lambda 950 UV/Vis spectrophotometer was used for recording the UV-Vis absorption spectra of the day in solution and adsorbed on TiO_2. The emission spectra were obtained using Jasco FP-6500, Japan spectrofluorometer. All electrochemical measurements were performed in a three-electrode system using Potentiostat/ Galvanostat (VoltaLab 40 model PGZ 301), employing a carbon electrode (Ø: 3 mm) as a working electrode, platinum column as a counter electrode, and an Ag/AgCl electrode as the reference electrode. All data were calibrated with respect to the ferrocene/ferrocenium system. The electrochemical measurments of 0.2 mM of the dye was elaborated in 0.1 M tetrabutylammonium hexafluorophosphate ($TBAPF_6$) in dichloromethane solution as the supporting electrolyte. The voltage is reported with respect to the normal hydrogen electrode (NHE) scale. MALDI-TOF/TOF-MS measurements were carried out using a 4800 Plus MALDI-ToF/ToF mass spectrometer (Applied Biosystems/MDS SCIEX, Foster City, CA, USA) equipped with a Nd: YAG pulsed laser (355 nm wavelength of <500 ps pulse and 200 Hz repetition rate). The 4000 Series Explorer software (V 3.5.3, Build 1017, 2007, Foster City, CA, USA) and the data explorer software (V 4.9, Build 115, 2007, Foster City, CA, USA) were used for analysis. Data acquisition was performed in the reflector positive ion mode. Each mass spectrum obtained was an average of 500 laser shots over the whole spot.

Synthesis of organic dye

4'-(bis(2',4'-dibutoxy-[1,1'-biphenyl]-4-yl)amino)-3,5-dimethoxy-[1,1'-biphenyl]-4-carbaldehyde

A 50 mL two neck schlenk flask equipped with a magnetic stir bar was charged with the donor (0.15 g, 0.18 mmol), 4-bromo-2,6-dimethoxybenzaldehyde (0.045g, 0.18 mmol), palladium acetate (6 mg, 0.009 mmol), tri-o-tolyl phosphine (11 mg, 0.037 mmol), potassium carbonate (0.08g, 0.55 mmol) and 20 ml degassed toluene/methanol (6:4). The reaction mixture was heated at 90 °C for 4 h. Next, the mixture was cooled down to room temperature and the solvent was removed under vacuum. The residue was washed with brine solution, extracted with ethyl acetate and dried over magnesium sulfate anhydrous. After the solvent was removed under vacuum, the product was purified by silica chromatograph using petrolumether: ethylacatate: dichloromethane: (9:0.075:4) as the eluent and a yellowish solid product was gained (0.10g, 65 % yield). ^{1}H NMR (400 MHz, CDCl3) δ 10.51 (s, 1H), 8.01 (s, 2H), 7.47 (d, *J* = 8.7 Hz, 4H), 7.27 (d, *J* = 4.7 Hz, 2H), 7.24 (d, *J* = 9.2 Hz, 2H), 7.19 (d, *J* = 8.3 Hz, 4H), 6.74 (d, *J* = 9.4 Hz, 3H), 6.60 – 6.50 (m, 4H), 3.99 (q, *J* = 12.6, Hz, 8H), 2.95 (s, 3H), 2.88 (s, 3H), 1.76 (m, 13H), 1.56 – 1.34 (m, 8H), 0.99 (t, *J* = 7.4 Hz, 6H), 0.93 (t, *J* = 5.4 Hz, 6H)ppm.^{13}C NMR (100 MHz, $CDCl_3$) δ 189.09, 162.68, 162.64, 162.43, 159.78, 157.11, 148.93, 145.51, 133.76, 133.31, 130.95, 130.44, 127.98, 124.28, 123.15, 123.02, 112.78, 108.11, 105.51, 102.40, 100.61, 68.29, 67.94, 56.53, 56.23, 36.61, 31.57, 31.52, 31.34, 19.47, 19.41, 14.00, 13.96 ppm.

(E)-3-(4'-(bis(2',4'-dibutoxy-[1,1'-biphenyl]-4-yl)amino)-3,5-dimethoxy-[1,1'-biphenyl]-4-yl)-2-cyanoacrylic acid (Z25)

A 50 mL one neck bottle flask equipped with a magnetic stir bar was charged with aldehyde (0.15 g, 0.18 mmol), 2-cyanoacetic acid (45 mg, 0.53 mmol) and 2-3 drops of piperdine were dissolved in 20 ml of chloroform under inert gas. The reaction mixture was refluxed for 4 h. After that the solvent was removed under reduced pressure. After the solvent was removed under vacuum, the product was purified by silica chromatograph using dichloromethane: methanol (9:1) as the eluent to obtain a brown solid product (0.11g, 60 % yields). ^{1}H NMR (400 MHz, Acetone) δ 8.36(s, 1 H), 7.62 (dd, *J* = 11.9, 8.5 Hz, 1H), 7.48 (t, *J* = 8.5 Hz, 4H), 7.25 (d, *J* = 8.3 Hz, 1H), 7.20 (d, *J* = 8.9 Hz, 1H), 7.13 (d, *J* = 8.0 Hz, 4H),6.92(d, *J* = 15.2 Hz, 1H), 6.84(d, *J* = 14.8 Hz, 1H), 6.62 (d, *J* = 7.6 Hz, 2H), 6.55 (dd, *J* = 17.5, 8.2 Hz, 2H), 4.00 (s, 3H), 3.93 (q, *J* = 21.2 Hz, 8H), 1.80 – 1.62 (m, 8H), 1.56 – 1.41 (m, 8H), 0.98 (t, *J* = 7.3 Hz, 6H), 0.93 – 0.89 (m, 6H)ppm. ^{13}C NMR (101 MHz, Acetone) δ 159.83, 157.04, 145.66, 133.78, 133.60, 130.66, 130.25, 127.82, 127.79, 123.83, 123.55, 122.61, 122.53, 105.83, 100.27, 67.88, 67.44, 55.62, 55.19, 31.27, 31.15, 19.16, 19.07, 13.32, 13.30 ppm. MS (MALDI-TOF) m/z calculated for $C_{58}H_{64}N_2O_8$: 916.4734; found, 916.4711 (Supporting information).

Device Fabrication and testing

Fluorine-doped tin oxide (FTO) glass substrates were cleaned in an ultrasonic bath using a detergent solution, deionized water and ethanol, respectively (each step 30 min long). The conducting glass substrates were pretreated by immersion in a 40 mM aqueous $TiCl_4$ solution at 70 °C for 20 min and then washed with ethanol

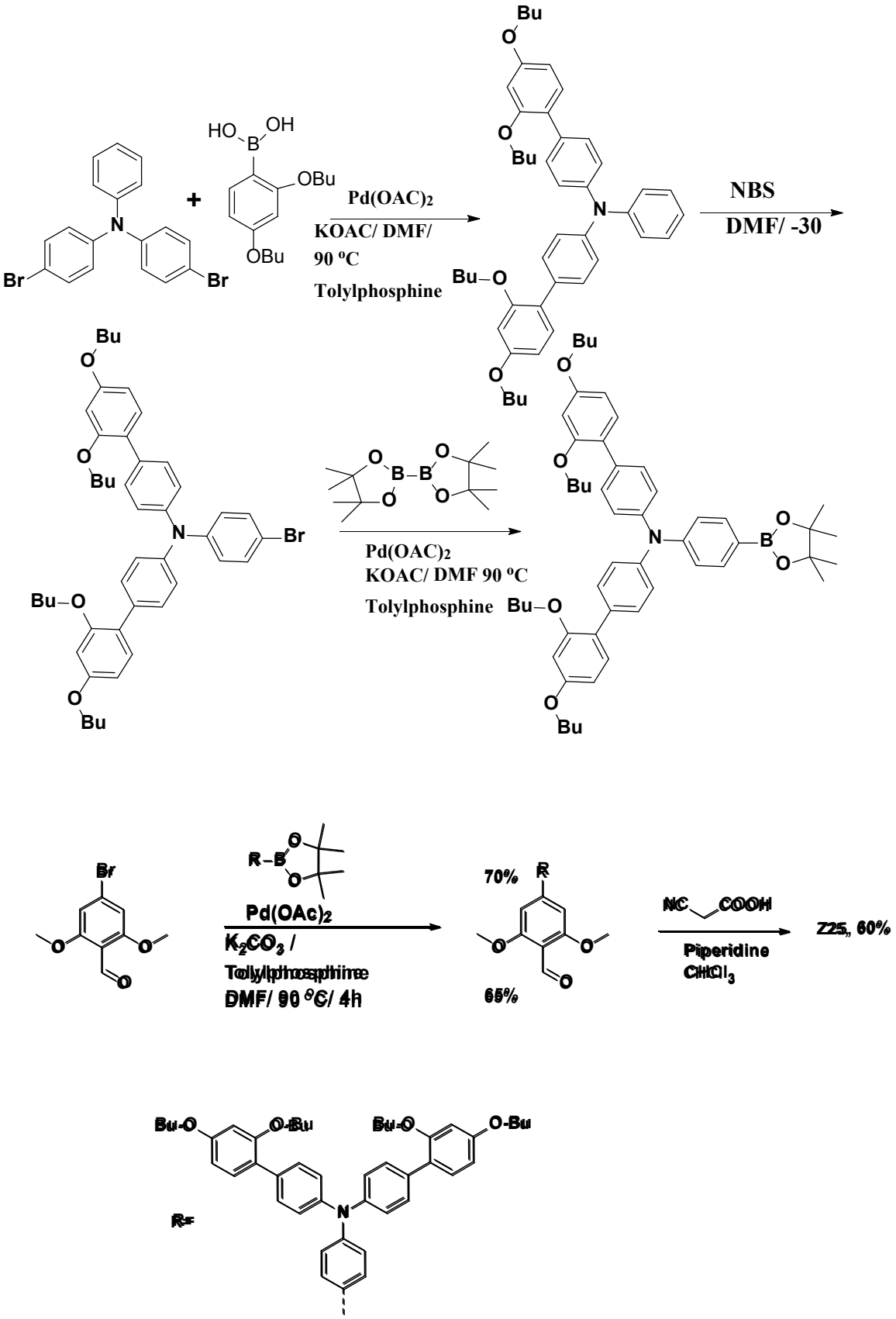

Scheme 1. Synthetic pathways of Z25 sensitizer

and dried with N_2. The triple TiO_2 layers on the FTO glass were prepared with an active area of 0.16 cm^2 by repeatedly screen printing TiO_2 paste (Nanoxide T/SP, Solaronix, Switzerland) and drying at 300 °C between deposition steps. After sintering, the thickness of the films was measured with a profilometer and was ~12 μm. Then, the electrodes were immersed in aqueous TiC_{l4}, rinsed as above and finally sintered at 450 °C for 30 min. When the temperature cooled to 80 °C, the electrodes were immersed into the dye bath containing 0.3 mM of Z25 dye along with chenodeoxycholic acid (0.3mM) in CH_2Cl_2 and kept at room temperature for 6 h. The photoanodes were then washed with ethanol to remove unabsorbed dye. Platinized FTO was purchased and used as a counter electrode. The Co-based electrolytes consist of: 0.22 M Co $(bpy)_3$ $(PF6)_2$, $Co(bpy)_3$ $(PF6)_3$, 0.1 M $LiClO_4$, and 0.2 M 4-*tert*-butylpyridine (TBP) in acetonitrile. The working electrode and the Pt counter-electrode were sealed with a 25 μm thick thermoplastic Surlyn (Meltonix 1170-25, Solaronix, Switzerland) under heating at 120 °C for a few seconds. An electrolyte solution was then injected into the cell through the hole presented in the counter electrode, and the cell was sealed with thermoplastic Surlyn and cover glass to avoid leakage of the electrolyte. The fabricated DSSCs based on Z25 dye were tested under AM 1.5 illumination (100 mW cm^{-2}) using a Keithley Model 2400 source meter. The light source was calibrated with a silicon reference cell before use.

Results and Discussion

Synthesis

The synthetic pathway of Z25 dye is shown in Scheme 1. The 2',4'-dibutoxy-N-(2',4'-dibutoxy-[1,1'-biphenyl]-4-yl)-N-(4-(4,4,5,5-tetramethyl-1,3,2-dioxaborolan-2-yl)phenyl)-[1,1'-biphenyl]-4-amine donor was prepared according to literature [43]. The precursor aldehyde was synthesized, in good yield (65%), via palladium-catalyzed Suzuki coupling reaction [44] of 4-bromo-2,6-dimethoxybenzaldehyde with the donor boronic ester with 1:1 molar ratio. Afterward, Z25 was synthesized in a yield of 60 % by Knoevenagel condensation of the aldehyde with 2-cyanoacetic acid in refluxing chloroform using drops of piperidine as catalyst.

Theoretical studies

The optimized geometry of Z25 dye is presented in Fig. 2 and its energetic properties are listed in Table 1. The calculations revealed that the bond length values of the C=O and the C-O in the carboxylate group are approximately 1.21 Å and 1.35 Å, respectively. The bond angle C-N-C was ~ 120°, which suggests that the dye has a

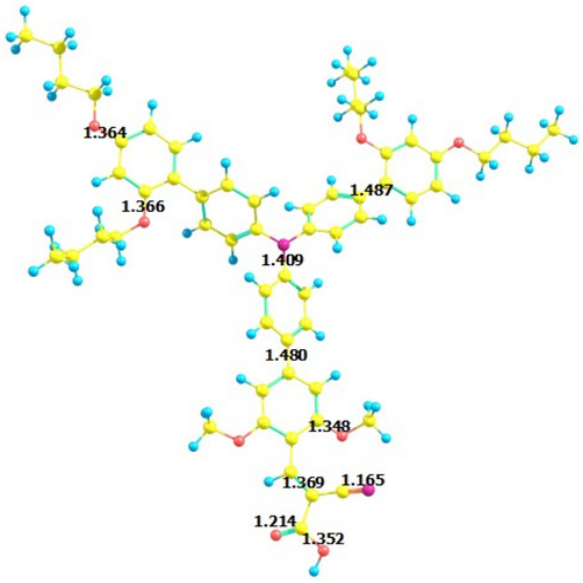

Fig. 2. Optimized geometry of Z25 dye and selected bond lengths shown in angstrom.

TABLE 1. Energetic properties of the studied dye: E_T= total energy, ΔE= E_{LMO}-E_{HOMO} and μ= the dipole moment, EA= electron affinity, IP= ionization potential, $E_{excitation}$= excitation binding energy, N_{Ex}= normalized excitation binding energy.

E_T (a.u.)	**-2959.2864**
E_{LUMO} (eV)	-2.3315
E_{HOMO} (eV)	-5.0320
ΔE (eV)	2.7005
μ (Deby)	11.6517
IP (eV)	5.9974
EA (eV)	15.0397
$E_{excitation}$ (eV)	0.2808
N_{Ex}	0.1040

trigonal planar geometry around the nitrogen atom without any distortion.

The value of the energy gap is of good value to allow the transition between the HOMO and the LUMO of the dye. Furthermore, the energy of the LUMO is lower than the energy of the conduction band of the anatase TiO_2, 45 which is frequently used as a semiconductor in DSSCs.46 The electronic excitation properties are given in Table 2 and the calculated absorption peaks of the dye are illustrated in Fig. 3. The excitation data shows two main peaks covering long range of wavelengths in the visible region and proving the dye to be good in DSSC. The frontier HOMO and LUMO distributions are given in Fig. 4 indicate that for the HOMO, the orbital distribution is around the orbitals of the N atom and π orbitals of the rings attached to it and for LUMO, the orbital distribution is around the π* orbitals of the anchoring group and the ring attached to it. This distribution affords a clear pathway for the charge transfer to the anchoring group and illustrates the opportunity of injection of charge carriers to the semiconductor.

Photophysical and Electrochemical properties

The UV-vis absorption and emission spectra of Z25 in CH_2Cl_2 are illustrated in Fig. 5a-b, and the related data are summarized in Table 3. The measured UV-vis spectrum was as expected from the computational TD-DFT and it shows two distinct absorption bands: the earlier band at λ= 370 nm due to the localized aromatic π-π* electronic

TABLE 2. Electronic excitation properties of Z25 dye, *f*= oscillator strength, *LHE*= light harvesting efficiency, *λ*= wavelength.

State no.	Main configuration	Coefficient	*f*	*LHE*	*λ* (nm)
S1	H → L	0.70450	0.5514	0.7191	512.43
S3	H-2 → L	0.66657	0.6330	0.7672	369.08
S5	H → L+1	0.55028	0.6008	0.7493	351.21

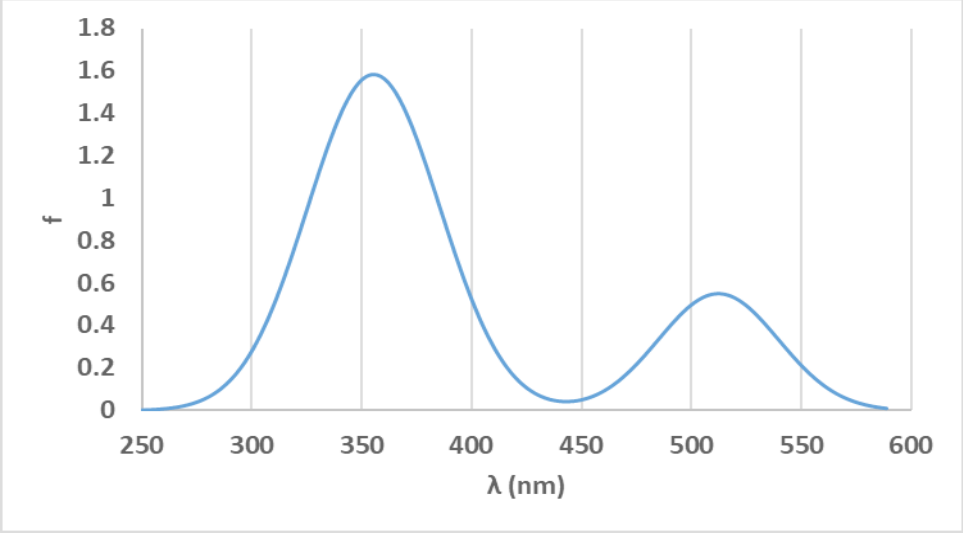

Fig. 3. Calculated absorption spectra for Z25 dye.

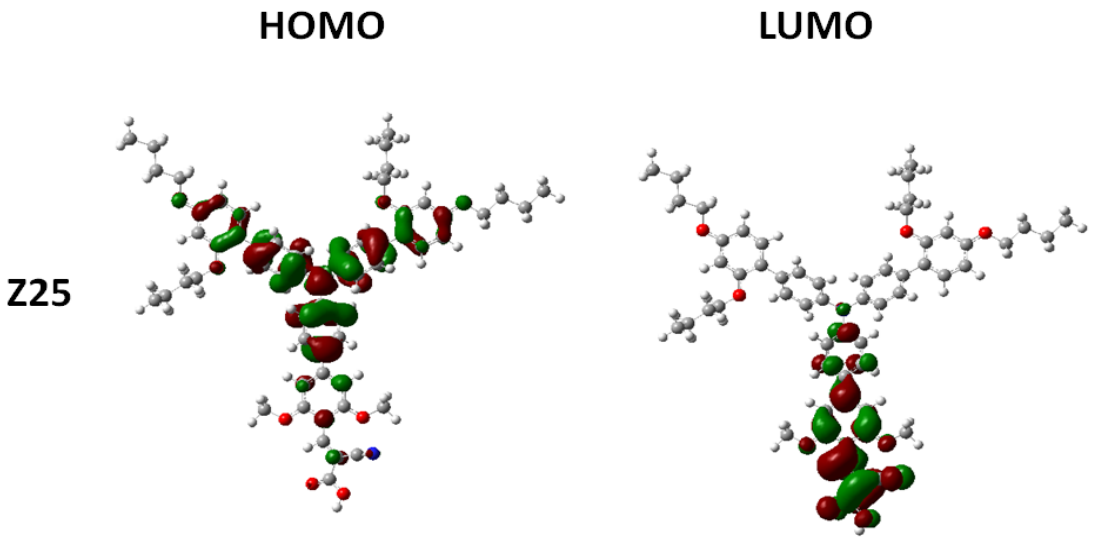

Fig. 4. HOMO and LUMO electronic distribution for Z25 dye

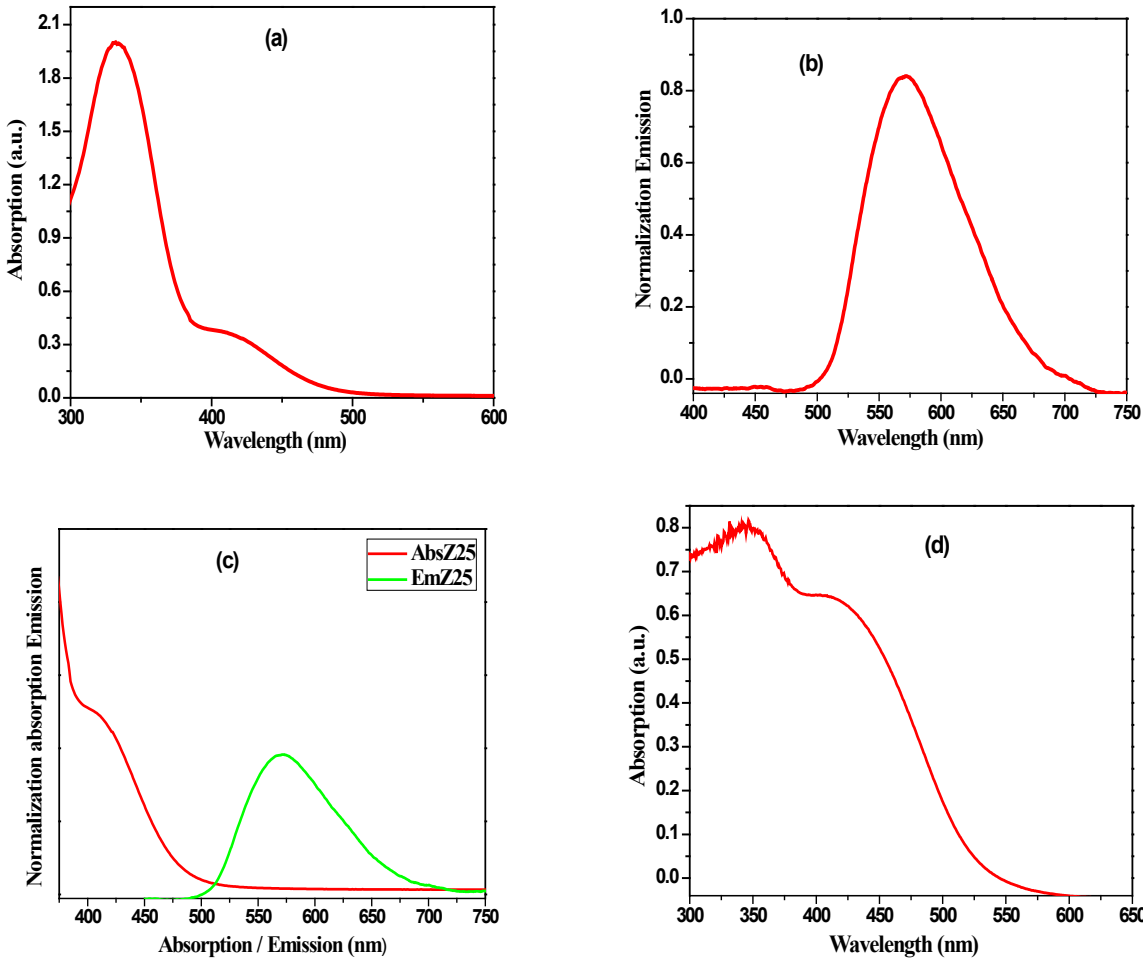

Fig. 5. a) Absorption spectra, b) Emission spectra, c) UV-Vis and Emission spectra of Z25 dye in CH_2Cl_2 and d) UV-visible absorption spectra of Z25 dye adsorbed on TiO_2.

transitions of the main conjugated skeleton, and the second band at 420 nm is related to the ICT transitions from the donor to the acceptor of the chromophore. In CH_2Cl_2, the dye shows intense red fluorescence with $\lambda_{em,\ max}$=573 nm due to the charge transfer to the electron accepting groups. The optical band gap energy (E0-0) of 25 assessed from the onset of the absorption and emission spectra (Fig. 5c) was 2.41 eV.

Figure 5d illustrates the absorption spectrum of Z25 adsorbed on TiO_2 film. Compared to the absorption spectrum in CH2Cl2 solution, the ICT band for Z25 sensitizer is broadened and red-shifted, indicating the formation of J-aggregation of the dye on the TiO_2 surface [47]. Figure 6 displays the cyclic voltammogram of Z25 dye and the corresponding data are depicted in Table 1. The dye exhibits two oxidation and reduction peaks

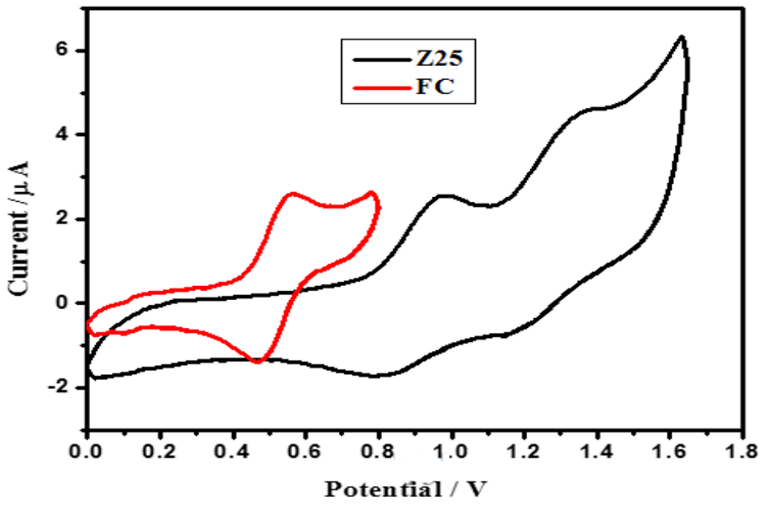

Fig. 6. Cyclic voltammograms of Z25 dye measured in CH_2Cl_2 solutions at room temperature.

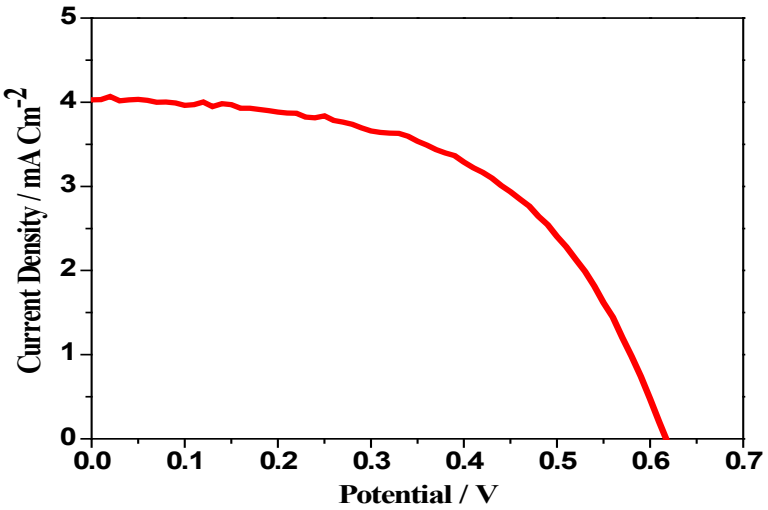

Fig. 7. J-V characteristics of the DSSCs devices based on Z25 dye and the $Co^{II/III}$ electrolyte.

TABLE 3. Absorption, emission and electrochemical data for the dye measured in CH_2Cl_2 solution.

Dye	$\lambda_{abs,\ max}$ (Ɛ) [nm(M^{-1} cm^{-1})]	$\lambda_{em,\ max}$	E_{HOMO} [a)] [V vs NHE]	$E_{0\text{-}0}$ [b)] [eV]	E_{ox} [c)] [V vs NHE]	E_{LUMO} [d)] [V vs NHE]
Z25	331(18371), 420 (8500)	573	1.00	2.41	0.87	-1.41

under the experimental conditions illustrated in experimental section. The initial peak around 0.87 V vs. NHE, is related to the HOMO level, while the other peak is due to the redox potential of the HOMO-1 orbital. The oxidation potential of the excited state of Z25 sensitizer is more negative than the conduction band edge of anatase TiO_2 (E_{CB} = −0.5 V vs. NHE) [48], and its ground state oxidation potential is more positive than the $Co^{II/III}$ (+0.56 V vs. NHE) [42] redox shuttle. Therefore, the synthesized dye is capable to act as sensitizer in DSSC devices where the dye can allow the electrons to be transferred from its LUMO into the conduction band of TiO_2 and enable the dye regeneration by electron transfer from cobalt ions in the electrolyte.

a) Calculated from the intersection of the normalized absorption and emission spectra; b) The ground-state oxidation potentials of the dyes were estimated under the following conditions: Pt as counter electrode and glass carbon working electrode. The electrolyte consisted of 0.2 m M dye and 0.05 M [Bu4 N]PF6 in dichloromethane. The reference Ag/Ag+ electrode was calibrated against an internal Fc/Fc + reference (E° (Fc/Fc+) = 0.63 V vs. NHE) c) Estimated by subtracting E0–0 from the oxidation potential [49].

Performance of the sensitizers in DSSCs

The Z25 sensitizer-based DSSC was fabricated along with the cobalt-based electrolyte and its photovoltaic performance was evaluated. Figure 7 demonstrates the current-voltage (*J-V*) curve of the fabricated DSSCs-based Z25 dyes under AM 1.5G illumination. The DSSC fabricated using Z25 dye showed the performance metrics of *JSC* = 4.0 mA cm^{-2}, *V*OC = 610 mV, FF = 0.53 and η = 1.3%.

Conclusion

The designed and synthesized dye was proved to be a good sensitizer in the visible region and it covers a long range of wavelengths with two peaks of high LHE in two different regions of the visible light. This proves that the 1,3-dimethoxybenzene was good as a π-linker that transfer charge effectively between the donor towards the acceptor and the anchoring group which will inject the charges easier to the semiconductor in the solar cell.

Acknowledgments

The Authors acknowledge the financial support from The Science and Technology Development Fund (STDF) provided by the Egyptian Government for chemical and measurements (Grant # 5415 from Nov. 2014to Feb. 2018).

Conflict of Interest

There is no conflict of interest

Data Availability

The data used to support the findings of this study are in separated file or available from the corresponding author upon request. (The supplementary data contains ^{1}HNMR, ^{13}CNMR and mass spectra of synthesized compound Z25)

References

1. Hagfeldt, A.; Graetzel, M., Light-induced redox reactions in nanocrystalline systems. *Chemical Reviews*, **95** (1), 49-68 (1995).

2. Zhang, S.; Yang, X.; Numata, Y.; Han, L., Highly efficient dye-sensitized solar cells: progress and future challenges. *Energy & Environmental Science*, **6** (5), 1443-1464 (2013).

3. Badawy, W. A., A review on solar cells from Si-single crystals to porous materials and quantum dots. *Journal of Advanced Research*, **6** (2), 123-132 (2015).

4. El-Ghetany, H.; Khattab, N., Mathematical Modeling for Performance Prediction of a Humidification–Dehumidification Solar Water Desalination System in Egypt. *Egyptian Journal of Chemistry*, **59** (2), 145-+ (2016).

5. Mahmoud, F.; Assem, Y.; Shehata, A.; Motaung, D., Synthesis and Characterization of MEH-PPV for Solar Cell Application. *Egyptian Journal of Chemistry*, **59** (5), 911-933 (2016).

6. Hagfeldt, A.; Boschloo, G.; Sun, L.; Kloo, L.; Pettersson, H., Dye-sensitized solar cells. *Chemical Reviews,* **110** (11), 6595-6663 (2010).

7. Wu, W.; Zhang, J.; Yang, H.; Jin, B.; Hu, Y.; Hua, J.; Jing, C.; Long, Y.; Tian, H., Narrowing band gap of platinum acetylide dye-sensitized solar cell sensitizers with thiophene π-bridges. *Journal of Materials Chemistry,* **22** (12), 5382-5389 (2012).

8. Liang, M.; Chen, J., Arylamine organic dyes for dye-sensitized solar cells. *Chemical Society Reviews,* **42** (8), 3453-3488 (2013).

9. Venkateswararao, A.; Thomas, K. J.; Li, C.-T.; Ho, K.-C., Functional tuning of organic dyes

containing 2, 7-carbazole and other electron-rich segments in the conjugation pathway. *RSC Advances*, **5** (23), 17953-17966 (2015).

10. Kim, B. G.; Chung, K.; Kim, J., Molecular Design Principle of All□organic Dyes for Dye□ Sensitized Solar Cells. *Chemistry-A European Journal,* **19** (17), 5220-5230 (2013).

11. Yen, Y.-S.; Chou, H.-H.; Chen, Y.-C.; Hsu, C.-Y.; Lin, J. T., Recent developments in molecule-based organic materials for dye-sensitized solar cells. *Journal of Materials Chemistry*, **22** (18), 8734-8747 (2012).

12. Ning, Z.; Fu, Y.; Tian, H., Improvement of dye-sensitized solar cells: what we know and what we need to know. *Energy & Environmental Science*, **3** (9), 1170-1181 (2010).

13. Wielopolski, M.; Kim, J.-H.; Jung, Y.-S.; Yu, Y.-J.; Kay, K.-Y.; Holcombe, T. W.; Zakeeruddin, S. M.; Grätzel, M.; Moser, J.-E., Position-Dependent Extension of π-Conjugation in D-π-A Dye Sensitizers and the Impact on the Charge-Transfer Properties. *The Journal of Physical Chemistry C*, **117** (27), 13805-13815 (2013).

14. Zhang, X.; Gou, F.; Zhao, D.; Shi, J.; Gao, H.; Zhu, Z.; Jing, H., π-Spacer effect in dithiafulvenyl-π-phenothiazine dyes for dye-sensitized solar cells. *Journal of Power Sources,* **324**, 484-491 (2016).

15. Yan, R.; Qian, X.; Jiang, Y.; He, Y.; Hang, Y.; Hou, L., Ethynylene-linked planar rigid organic dyes based on indeno [1, 2-b] indole for efficient dye-sensitized solar cells. *Dyes and Pigments*, **141**, 93-102 (2017).

16. Torres, É.; Sequeira, S.; Parreira, P.; Mendes, P.; Silva, T.; Lobato, K.; Brites, M. J., Coumarin dye with ethynyl group as π-spacer unit for dye sensitized solar cells. *Journal of Photochemistry and Photobiology A: Chemistry*, **310**, 1-8 (2015).

17. Hua, Y.; Lee, L. T. L.; Zhang, C.; Zhao, J.; Chen, T.; Wong, W.-Y.; Wong, W.-K.; Zhu, X., Co-sensitization of 3D bulky phenothiazine-cored photosensitizers with planar squaraine dyes for efficient dye-sensitized solar cells. *Journal of Materials Chemistry A*, **3** (26), 13848-13855 (2015).

18. Sharmoukh, W.; Attanzio, A.; Busatto, E.; Etienne, T.; Carli, S.; Monari, A.; Assfeld, X.; Beley, M.; Caramori, S.; Gros, P. C., 2, 5-Dithienylpyrrole (DTP) as a donor component in DTP–π–A organic sensitizers: photophysical and photovoltaic properties. *RSC Advances*, **5** (6), 4041-4050 (2015).

19. Hao, Y.; Tian, H.; Cong, J.; Yang, W.; Bora, I.; Sun, L.; Boschloo, G.; Hagfeldt, A., Triphenylamine Groups Improve Blocking Behavior of Phenoxazine Dyes in Cobalt□ Electrolyte□Based Dye□Sensitized Solar Cells. *Chem. Phys. Chem.,* **15** (16), 3476-3483 (2014).

20. Joly, D.; Pelleja, L.; Narbey, S.; Oswald, F.; Meyer, T.; Kervella, Y.; Maldivi, P.; Clifford, J.; Palomares, E.; Demadrille, R., Metal-free organic sensitizers with narrow absorption in the visible for solar cells exceeding 10% efficiency. *Energy & Environmental Science*, **8** (7), 2010-2018 (2015).

21. Gupta, K.; Singh, S. P.; Islam, A.; Han, L.; Chandrasekharam, M., Simple fluorene based triarylamine metal-free organic sensitizers. *Electrochimica Acta*, **174**, 581-587 (2015).

22. Numata, Y.; Ashraful, I.; Shirai, Y.; Han, L., Preparation of donor–acceptor type organic dyes bearing various electron-withdrawing groups for dye-sensitized solar cell application. *Chemical Communications*, **47** (21), 6159-6161 (2011).

23. Liang, M.; Xu, W.; Cai, F.; Chen, P.; Peng, B.; Chen, J.; Li, Z., New triphenylamine-based organic dyes for efficient dye-sensitized solar cells. *The Journal of Physical Chemistry C*, **111** (11), 4465-4472 (2007).

24. Cao, D.; Peng, J.; Hong, Y.; Fang, X.; Wang, L.; Meier, H., Enhanced performance of the dye-sensitized solar cells with phenothiazine-based dyes containing double D− A branches. *Organic Letters*, **13** (7), 1610-1613 (2011).

25. Ambrosio, F.; Martsinovich, N.; Troisi, A., Effect of the anchoring group on electron injection: theoretical study of phosphonated dyes for dye-sensitized solar cells. *The Journal of Physical Chemistry C*, **116** (3), 2622-2629 (2012).

26. Ali, B. A.; Allam, N. K., Propping the optical and electronic properties of potential photo-sensitizers with different π-spacers: TD-DFT insights. *Spectrochimica Acta Part A: Molecular and Biomolecular Spectroscopy*, **188**, 237-243 (2018).

27. W. Kohn, N. L., *Rev. Mod. Phys.*, **71**, 1253–1266 (1999).

28. Gaussian 09, R. E., M. J. Frisch, G. W. Trucks, H. B. Schlegel, G. E. Scuseria, M. A. Robb, J. R. Cheeseman, G. Scalmani, V. Barone, B.

Mennucci, G. A. Petersson, H. Nakatsuji, M. Caricato, X. Li, H. P. Hratchian, A. F. Izmaylov, J. Bloino, G. Zheng, J. L. Sonnenberg, M. Hada, M. Ehara, K. Toyota, R. Fukuda, J. Hasegawa, M. Ishida, T. Nakajima, Y. Honda, O. Kitao, H. Nakai, T. Vreven, J. A. Montgomery, Jr., J. E. Peralta, F. Ogliaro, M. Bearpark, J. J. Heyd, E. Brothers, K. N. Kudin, V. N. Staroverov, R. Kobayashi, J. Normand, K. Raghavachari, A. Rendell, J. C. Burant, S. S. Iyengar, J. Tomasi, M. Cossi, N. Rega, J. M. Millam, M. Klene, J. E. Knox, J. B. Cross, V. Bakken, C. Adamo, J. Jaramillo, R. Gomperts, R. E. Stratmann, O. Yazyev, A. J. Austin, R. Cammi, C. Pomelli, J. W. Ochterski, R. L. Martin, K. Morokuma, V. G. Zakrzewski, G. A. Voth, P. Salvador, J. J. Dannenberg, S. Dapprich, A. D. Daniels, Ö. Farkas, J. B. Foresman, J. V. Ortiz, J. Cioslowski, and D. J. Fox, 356 Gaussian, Inc., Wallingford CT, (2009).

29. Becke A. D. , *J. Chem. Phys.*, **98**, 5648 (1993).

30. Lee C.; Yang, W.; and Parr R. G. , *Phys. Rev. B: Condens. Matter Mater. Phys.,* **37**, 785 (1988).

31. Miehlich B.; Savin A.; Stoll, H.; and Preuss H., *Chem. Phys. Lett.*, **157**, 200 (1989).

32. Martin J. M.; El-Yazal, J.; and Francois J., *Mol. Phys.*, 86, 1437 (1995).

33. Jr. Dunning; Thom H., *The Journal of Chemical Physical*, **90** (2), 1007-1023 (1989).

34. Bernini C.; Zani L.; Calamante M.; Reginato G.; Mordini A.; Taddei M.; Basosi R.; Sinicropi A., *Journal of Chemical Theory and Computation*, **10** (9), 3925-3933 (2014).

35. Wielopolski M.; Marszalek M.; Brunetti F. G.; Joly D.; Calbo J.; Aragó J.; Moser J-E.; Humphry-Baker; R., Zakeeruddin Sh. M.; Delgado J. L, *Journal of Materials Chemistry C*, **4** (17), 3798-3808 (2016).

36. Hehre W. J.; Ditchfield R.; and Pople J. A., *J. Chem. Phys.*, **56**, 2257 (1972).

37. http://www.chemcraftprog.com.

38. Gauss View, V.; R. Dennington; and, T. K.; J. Millam; Semichem Inc., Shawnee Mission, KS. 2009.

39. Sharmoukh W.; Hassan W. MI.; Gros Ph. C.; Allam N. K., *RSC Advances*, **6** (73), 69647-69657 (2016).

40. Sengul O.; Boydas E. B.; Pastore M.; W. Sharmoukh; Ph. C.Gros; S. Catak; A. Monari, *Theoretical Chemistry Accounts*, **136** (6), 67 (2017).

41. Nalwa H.S., Handbook of advanced electronic and photonic materials and devices Academic: San Diego, (2001).

42. Feldt S. M.; Gibson E. A.; Gabrielsson E.; Sun L.; Boschloo G.; Hagfeldt A., *J. AM. CHEM. SOC.*, **132**, 16714–16724 (2010).

43. Erik G.; Hanna E.; Sandra, F.; Haining, T.; Gerrit, B.; Anders, H.; Licheng, S., Convergent/ Divergent Synthesis of a Linker□Varied Series of Dyes for Dye□Sensitized Solar Cells Based on the D35 Donor. *Adv. Energy Mater.*, **3**, 1647–1656 (2013).

44. Suzuki, A., Recent advances in the cross-coupling reactions of organoboron derivatives with organic electrophiles, 1995–1998. *Journal of Organometallic Chemistry*, **576**, 147–168 (1999).

45. Scanlon D. O.; Dunnill C. W.; Buckeridge J.; Shevlin, S. A.; Logsdail A. J.; Woodley S. M.; Catlow C. R. A.; Powell M. J.; Palgrave R. G.; I. Parkin P., *Nature Materials*, **12** (9), 798-801 (2013).

46. Kałużyński P.; Maciak E.; Herzog T.; Wójcik M. *International Society for Optics and Photonics:* pp 100310N-100310N-8 (2016).

47. He, J.; Wu, W.; Hua, J.; Jiang, Y.; Qu, S.; Li, J.; Long, Y.; Tian, H., Bithiazole-bridged dyes for dye-sensitized solar cells with high open circuit voltage performance. *Journal of Materials Chemistry*, **21** (16), 6054-6062 (2011).

48. Zhang, X.; Mao, J.; Wang, D.; Li, X.; Yang, J.; Shen, Z.; Wu, W.; Li, J.; Ågren, H.; Hua, J., Comparative study on pyrido [3, 4-b] pyrazine-based sensitizers by tuning bulky donors for dye-sensitized solar cells. *ACS Applied Materials & Interfaces*, **7** (4), 2760-2771 (2015).

49. Gabrielsson, E.; Ellis, H.; Feldt, S.; Tian, H.; Boschloo, G.; Hagfeldt, A.; Sun, L., Convergent/ Divergent Synthesis of a Linker□Varied Series of Dyes for Dye□Sensitized Solar Cells Based on the D35 Donor. *Advanced Energy Materials*, 3 (12), 1647-1656 (2013).

(*Received* 28/6/2018;
accepted 10/9/2018)

الهندسة الجزيئية لمركب صبغي من النوع معطي- باي- مستقبل للالكترونات يعتمد على1 و-3 داي ميثوكثي بنزين للإستخدام في خلايا الطاقة الشمسية الصبغية

وليد شرموخ[١]، زينب محمد حسن[٢]، بسنت أحمد علي[٣]، محمد محمود النجار[١]، حنان عبد الهادي موسى[١]، عمار أحمد لبيب[١]

[١]قسم الكيمياء غير العضوية - المركز القوي للبحوث - شارع التحرير- الدقي ١٢٦٢٢ - الجيزة - مصر.

[٢]قسم الكيمياء - جامعة الفيوم - كلية العلوم - الفيوم - مصر.

[٣]معمل مواد الطاقة - كلية العلوم والهندسة - الجامعة الأمريكية بالقاهرة - القاهرة الجديدة ١١٨٣٥- مصر.

تم تحضير مركب عضوي جديد يشتمل على مركب D35 كوحدة مانحة ، 1.3-dimethoxybenzene باعتباره رابط جديد يمكن ترابطه بسطح TiO_2 ، كما تم توصيف المركب باستخدام جهاز طيف الاشعة المرئية والفوق بنفسجية وجهاز الرنين المغناطيسى ومطياف الكتلة. كما تمت دراسة الخواص الفيزوضوئية و الكهروكيميائية ، وكذلك الأداء الضوئي لهذه الصبغة ، لتقييم تأثير الرابطة π الجديدة على كفاءة تحويل القدرة (PCE). وقد لوحظ تحسين في التكوين الهندسي للمحسسات من خلال حسابات الكثافة النظرية الوظيفية (DFT) للحصول على رؤية عميقة في البنية الجزيئية والخصائص الإلكترونية. وتم الحصول على قياسات كهروضوئية للمركب الجديد عند استخدامه في تكوين الخلية الصبغية DSSC كالتالى :

$JSC = 4.0$ mA cm^{-2} و $VOC = 610$ mV و $FF = 0.53$ و $\eta = 1.3$ ٪ تحت إضاءة AM 1.5 G القياسية.